Thermotropic Phase Behavior of Multilamellar Membranes of Dioleoylphosphatidylcholine

Yu-Dong Zhang, Ying Lu, Shu-Xin Hu,* and Ming Li

Beijing National Laboratory for Condensed Matter Physics and Key Laboratory of Soft Matter Physics, Institute of Physics, Chinese Academy of Sciences, Beijing 100190, China

Received: October 11, 2009; Revised Manuscript Received: January 7, 2010

We use the X-ray diffraction method to examine the thermotropic phase behavior of multilamellar membranes of dioleoylphosphatidylcholine. We find that when the temperature is reduced from room temperature to below 0 °C, both the lipid bilayers and the amount of water in the bilayers increase. But the interbilayer distance descends abruptly at a certain temperature between −6 and −15 °C, the actual value depending on the relative humidity of the atmosphere, solely due to the thinning of the water layer, d_w. There are several L_α and L_c phase coexistence states both in the cooling process and in the heating process. In the cooling process, only a part of the lipid molecules accomplish the L_α-to-L_c main phase transition at −16 °C, with the rest of the lipids being frozen down to a very low temperature. In the heating process, however, these frozen lipid molecules are able to move to complete the L_α-to-L_c main phase transition at −12 °C. The reverse of the main phase transition begins at −9 °C and is completed at −5 °C, after which the water is absorbed into the lipid bilayer to increase the thickness of the water layer, while the thickness of the lipid membranes remain unchanged. This process continues until all the ice on top of the samples melts.

1. Introduction

The thermotropic phase behavior of biological membranes is of great interest.[1,2] For instance, the biorelevant liquid crystalline phase, also known as the fluidic phase or L_α phase, is essential to maintain the membranes' normal functions, whereas the less fluidic gel phase (L_β phase) and subgel phase (L_c phase) are not compatible with these functions.[3,4] By definition, the hydrocarbon chains of the lipid molecules in the L_α phase show a disordered gauche conformation, and there is no long-range order within the bilayers. In contrast, the hydrocarbon chains in the L_β phase show an extended trans conformation. The lipid molecules are two-dimensionally ordered but show no interlayer correlations. The straight hydrocarbon chains are three-dimensionally ordered in the L_c phase. Unsaturated phospholipids are essential constituents of cell membranes. Increasing the degree of unsaturation of the phospholipids has been commonly applied by plants and microorganisms to adapt to low temperature conditions.[5,6] Dioleoylphosphatidylcholine (DOPC) is often chosen as the model lipid because its liquid crystalline phase persists down to about −20 °C, just like most of the biological membranes.[7] A systematic thermal analysis of DOPC has been carried out using the differential scanning calorimetry method, and a useful phase diagram of the DOPC−water system was obtained.[8] The DOPC−water system undergoes a transition from the "L_α + water" state, via the "L_α + ice" state, to the "L_c + ice" state as the temperature is reduced from room temperature to below 0 °C. However, structural information is still needed to have a better understanding of the phase behavior of lipids.

X-ray diffraction has become an important technique to study the phase behavior of lipids. It has been used by Gleeson et al. to study DOPC membranes.[9] The lipids and water were mixed in an X-ray capillary to form the lamellar phase in their study. The results showed that ice forms at −12 °C, and the L_α phase persists down to −16 °C. However, many details about the phase behaviors are still unclear. The structural information from their powderlike samples is very limited because too few Bragg peaks could be measured. To get more accurate information on the thermotropic phase behaviors of DOPC, we prepared mulitlamellar membranes of DOPC on solid supports. The lipid bilayers are all parallel to the surface of the solid support so that many Bragg peaks are readily observable, providing more information about the structure of the lipid−water system.

2. Materials and Methods

DOPC (1,2-dioleoyl-*sn*-glycero-3-phosphatidylcholine) was purchased from Avanti Polar Lipid (Birmingham AL) and used without further purification. The samples were prepared using the drop-casting method, as before.[10−13] Briefly, DOPC was dissolved into mixed methanol−chloroform solvent (1:1, v/v) to get a solution with a concentration of 50 mg/mL. The solution was then pipetted onto silicon substrates, which were made hydrophilic according to the procedure of Hu et al.[10] The solution spread spontaneously, and the solvent evaporated slowly. After that, the samples were kept in a desiccator overnight to remove the organic solvent completely.

A two-chamber sample cell, with which we could control the temperature and the relative humidity (RH) of the atmosphere surrounding the sample,[14] was used in the experiments. The sample was located at the bottom of the inner chamber, with a sponge on the top to control the RH by adjusting the amount of water and glycerol in the sponge according to the ASTM standards.[15] The inner chamber was sealed to ensure that the RH was constant during the experiments. The temperature of the chamber was controlled by cycling an antifreeze liquid from a refrigerated bath. A thermocouple was mounted in the inner chamber to monitor the temperature. The sample was given enough time to equilibrate at each temperature.

The low-angle X-ray diffraction (XRD) experiments were performed on a Bruker D8-Advance diffractometer. From the Bragg peaks of the X-ray diffraction, we can directly obtain

* Corresponding author. Fax: (+86)-10-82640224. E-mail: hushuxin@aphy.iphy.ac.cn.

10.1021/jp909739y
Published on Web 01/26/2010

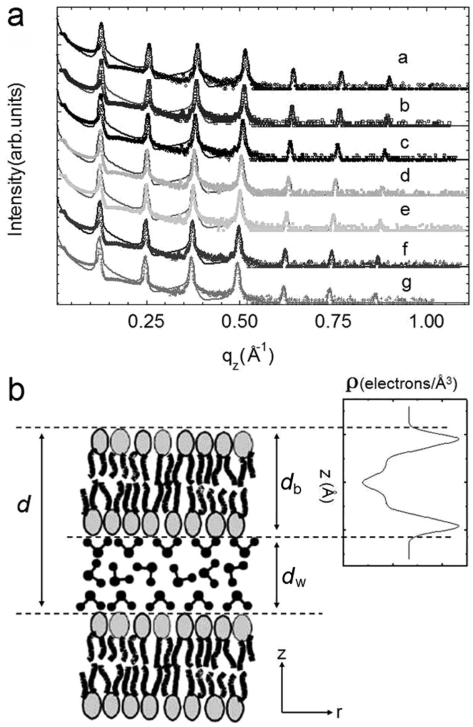

Figure 1. (a) XRD patterns of a sample in the initial cooling process from 20 to 0 °C. The solid lines are calculated XRD patterns according to the refined EDP of the samples. (b) Scheme showing how to separate an interbilayer distance into the thickness of the lipid bilayer and the thickness of the water layer.

the interbilayer distance of the membrane systems. The electron density profiles (EDP) of the lipid bilayers in different phases are reconstructed using a method proposed by Salditt et al.[10,11] Briefly, the EDP of a bilayer can be refined from the XRD data via

$$\rho(z) = \sum_{1}^{M} f(q_m) \cos(2\pi m z/d) \qquad (1)$$

where $f(q_m)$ is the form factor of the bilayer, d is the interbilayer distance of the multilamellar membrane system, and m running from 1 to M is the index of the Bragg peaks. The magnitudes of $f(q_m)$ are determined from the intensities at the Bragg peaks,

$$I(q) \propto |\sum_{0}^{N} f_n e^{iqnd}|^2/q^2 \qquad (2)$$

where $f_0 = f_S$ is the reflection of the substrate and $f_n = f(q)$ exp $(-idq/2)$. Due to the mirror plane symmetry of the bilayers, the phases of $f(q_m)$ are reduced to their positive/negative signs only, facilitating the phase problem enormously. The phases and zero crossings of the form factor are determined as described. A set of X-ray patterns of the sample during the cooling process are shown in Figure 1a, from which we can obtain the EDP of the membranes, such as the one shown in Figure 1b, which can be separated into a lipid bilayer with a thickness d_b and a water layer with a thickness d_w.[16]

3. Results and Discussion

The main result is depicted in Figure 2. It records the measured interbilayer distance of the multilamellar sample as a function of temperature at RH = 95%. The details of the phase behavior may differ from this typical curve at other RH values. The differences will be mentioned when necessary. We present in the following the details of the thermotropic phase behavior of the DOPC membranes following the "cooling−heating" route; namely, first from point A to point E, then from point E to point I in Figure 2.

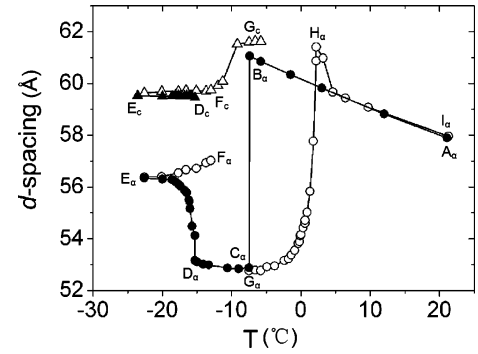

Figure 2. Temperature dependence of the interbilayer distance of the DOPC multilayered membranes at 95% RH. The solid symbols represent the cooling process, and the hollow symbols represent the heating process. The L_α phase is represented by circles, and the L_c phase is represented by triangles. The capital letters mark the states of the sample discussed in the text, with the subscripts indicating the specific phases: α for the L_α phase and c for the L_c phase.

3.1. The Linear Swelling (from A_α to B_α in Figure 2). As the temperature is reduced from room temperature to below 0 °C, the interbilayer distance of the multilamellar membranes increases linearly (from A_α to B_α in Figure 2). The linear trend of the curve was also observed in some other phospholipid systems. For instance, Mason et al. and Pabst et al. found the linear trend of the temperature dependence in various phosphatidylethanolamine and phosphatidylcholine systems when they were studying the critical swelling near the main phase transitions.[17,18] Pabst et al. attributed the linear swelling to a continuous reduction of the gauche isomers, pictured by the stretching-out of the hydrocarbon chains of the lipid bilayers. However, the possibility of the increase in water thickness remains unexamined. By analyzing the X-ray diffraction data, we obtained the EDP, such as the one shown in Figure 1b, from which we can estimate both the thickness of the water layer and the thickness of the lipid bilayer. As shown in Figure 3, the increment of the interbilayer distance Δd arises not only from the thickening of the lipid bilayer, Δd_b, but also from the thickening of the water layer, Δd_w. The increment rate of Δd_b is almost constant, 0.07 Å/°C, independent of the RH. However, the increment rate of Δd_w depends strongly on the RH. It increases from 0.01 Å/°C at RH = 75% to 0.05 Å/°C at RH = 100%. We adopt a *softening* mechanism to explain the phenomenon. The same mechanism has been used to explain the critical swelling in the vicinity of the main phase transition temperature, T_m.[19,20] It says that the expansion of the water layers arises from the enhancement of the repulsion between the adjacent bilayers because of the increased thermal undulations. Since we observed both the thickening of the lipid bilayers and the thickening of the water layers, the two different mechanisms (the stretching-out model and the softening model) might work simultaneously in the swelling process.

3.2. Cooling-Induced Dehydration (from B_α to C_α in Figure 2). The interbilayer distance increases until the temperature is lowered to about −7.5 °C, at which the interbilayer distance descends abruptly (from B_α to C_α in Figure 2).[9] The temperature at which the interbilayer distance descends varies

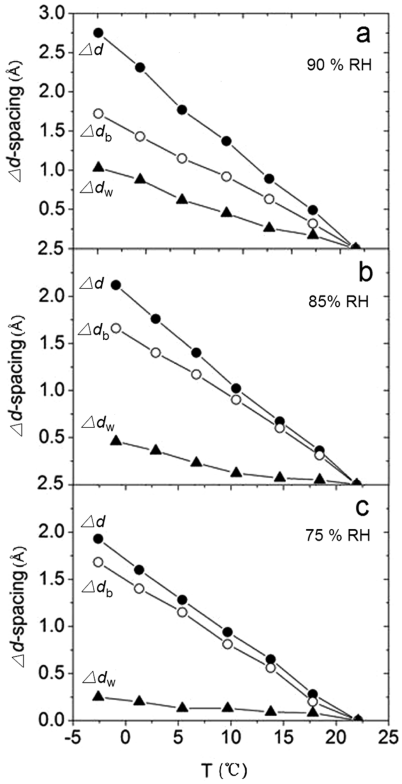

Figure 3. Temperature dependence of the increments of interbilayer distance (dots), the thickness of the bilayer (circles), and the thickness of the water layer (triangles) with respect to the values at 22 °C at different RH: (a) 90%, (b) 85%, and (c) 75%.

with the RH of the atmosphere. It moves from −6 °C at RH = 100% to −15 °C at RH = 60% in our experiments. The EDPs reveal that the decrease in the interbilayer distance is due solely to the thinning of the water layer, d_w, with the thickness of the lipid layer d_b being almost constant before and after the transition point. The thickness of the remaining water layers in the bilayers is estimated to be about 3 Å, corresponding to about one molecular layer of water. We currently do not know whether the remaining water is in the liquid or solid state. Answering this question requires an accurate definition of the structure of ice and water in such a thin space and more elaborate experimental work as well. Nevertheless, the thinning of the water layer means that the water between the lipid bilayers drains out of the sample in the cooling process. Meanwhile, we directly observed the morphological changes of the sample surface from the windows of the sample container. A few ice hills appeared on the surface of the sample after the interbilayer distance dropped.

The draining of the water eliminates all the differences arising from the differences in the RH at the beginning of the experiments. Whatever the initial RH is and however high the interbilayer distance can reach before the water drains, the interbilayer distances of all the studied systems become the same (53.1 ± 0.1 Å) after the water drains. This value corresponds to a system with the fewest water molecules incorporated in the lipid bilayers. The interbilayer distance remains almost constant upon further cooling until it leaps up again at −15.4 ± 0.9 °C at which the main phase transition occurs (from C_α to D_α in Figure 2).

3.3. The Main Phase Transition (from D_a to E_a in Figure 2). It was reported that the main phase transition of DOPC is directly from the lamellar liquid crystalline phase, L_α, to the lamellar crystalline phase, L_c, without passing through a lamellar gel phase, L_β.[21] The phase transition occurs at −15.4 ± 0.9 °C in our system (D_α and D_c in Figure 2), similar to that reported by Gleeson et al.[9] As can be seen from Figure 4, the main change in the XRD patterns is the emergence of a set of wide peaks that belong to the L_c phase when the temperature is reduced from −16.0 to −22.6 °C. The thickness of the bilayers in the L_α phase increases with the emergence of these wide peaks. However, it approaches a limit of 56.2 ± 0.2 Å and remains constant until the lowest temperature we can reach in our experiments (−22.6 °C, E_α in Figure 2). The narrow peaks of the L_α phase persist down to this temperature.

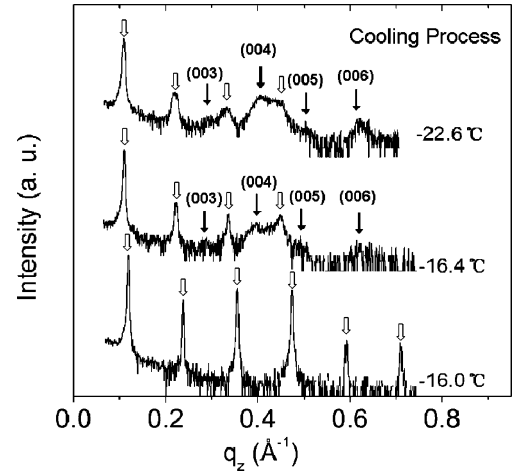

Figure 4. XRD patterns of the sample at −16.0, −16.4, and −22.6 °C in the cooling process (from D_α to E_α in Figure 2). The emerging wide peaks are from the L_c phase. These peaks are indexed according to the pattern of a fully developed L_c phase (see Figure 6) and marked by the black arrows. The peaks of the L_α phase are marked by the white arrows.

3.4. Reverse of the Main Phase Transition (from E to F and Then to G in Figure 2). The thickness of the lipid layers in the L_α phase increases again when the heating process is started from the lowest temperature, but the thickness of the lipid bilayers in the L_c phase remains almost constant until the temperature is increased to −13.0 °C (near F_c in Figure 2). Above this temperature, the L_α phase eventually begins to fade out (Figure 5), and the thickness of the lipid bilayers in the L_c phase increases rapidly. The L_α phase disappears completely and the thickness of the lipid layers in the L_c phase reaches its highest value at −12.0 °C. Only at this point is the transition from L_α to L_c completed.

The reverse of the main phase transition, in which the Bragg peaks of the L_α phase come back and the peaks of the L_c phase fade out, is observed from −9.2 to −4.9 °C (see Figure 6 and the routine from G_c to G_α in Figure 2). The thickness of the bilayers in the L_c phase remains the highest, and that in the emerging L_α phase goes directly to its lowest value in this process.

3.5. The Melting of Ice (from G_a via H_a to I_a in Figure 2). After the reverse main phase transition from L_c to L_α (from G_c to G_α in Figure 2), the interbilayer distance increases rapidly from 52.8 ± 0.1 to 61.6 ± 0.1 Å (from G_a to H_a in Figure 2). The increase in the interbilayer distance is mainly due to the thickening of the water layer, whereas the thickness of the lipid bilayer remains almost constant and even decreases a little bit (possibly due to the introduction of gauche isomers to the chains; see Figure 7). We visually observed the melting of the ice on the sample surface through the window of the sample chamber. After the ice on the surface melts, the excess water penetrates into the sample so that the bilayers hold much more water than

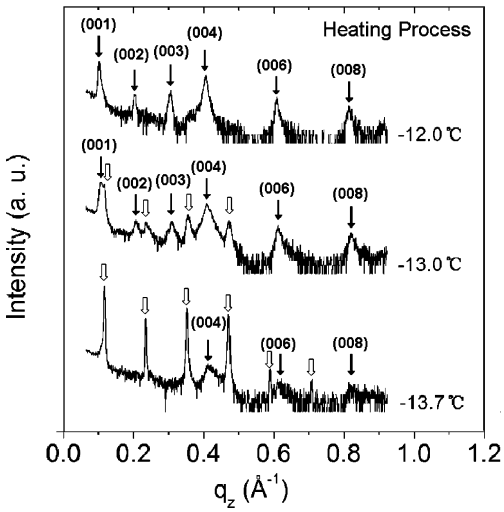

Figure 5. XRD patterns of the membrane at −13.7, −13.0, and −12.0 °C in the heating process (around F_c in Figure 2). The narrow peaks of the L_α phase fade out, and the wide peaks of the L_c phase develop into a complete set of peaks in this process. The peaks of the L_c phase are indexed and marked by black arrows. The peaks of the L_α phase are marked by white arrows.

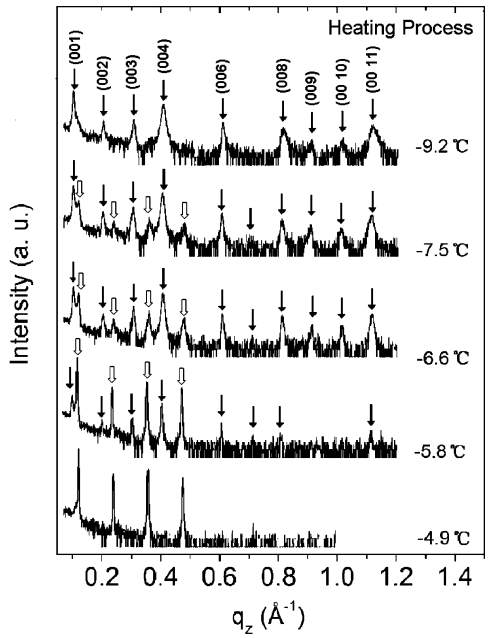

Figure 6. XRD patterns of the membranes at −9.2, −7.5, −6.6, −5.8, and −4.9 °C in the heating process, following the routine from G_c to G_α in Figure 2. The peaks of the L_c phase disappear and the peaks of the L_α phase come back in this process. The peaks of the L_c phase are marked by black arrows; the peaks of the L_α phase are marked by white arrows. For the sake of clearance, only the peaks of the L_c phase at −9.2 °C are indexed.

they did at the same temperature in the cooling process. This also explains why, after the ice melts, the interbilayer distance is higher in the heating process than in the cooling process at the same temperature (Figure 2).

4. Conclusion

The alignment of the lipid bilayers on solid supports has enabled us to examine the thermotropic phase behavior of the DOPC phospholipids in detail by using the X-ray diffraction method. Three main conclusions can be made: (1) When the sample is cooled from room temperature to the point above the

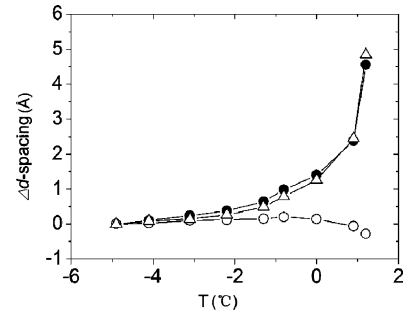

Figure 7. Temperature dependencies of the increments of the interbilayer distance (Δd, dots), the bilayer thickness (Δd_b, circles), and the water layer thickness (Δd_w, triangles) in the route from G_α to H_α in Figure 2.

L_α−ice coexistence state, both the lipid layer and the water layer are thickened. The alkyl chains themselves are elongated by about 0.85 Å, independent of the RH of the atmosphere, resulting in a thickening of the lipid bilayers by abou 1.7 Å. In contrast, the increment of the water layer thickness varies from about 0.3 Å at RH = 75% to about 1.3 Å at RH = 100%. The final thickness of the water layer is about 11 Å right above the cooling-induced dehydration point at RH = 100%. The alkyl chains are fully straightened with an increase in thickness by 8.6 ± 0.2 Å only after the main phase transition is completed. (2) The abrupt decrease in interbilayer distance is due solely to the thinning of the water layer, d_w, with an ∼3-Å-thick water layer remaining between the bilayers. Whether they are in the form of water or ice is currently unclear. (3) The temperature of the L_c-to-L_α phase transition is much higher than that of the L_α-to-L_c phase transition, indicating a hysteresis in the main phase transition. As a result, several L_α and L_c phase coexistence stages are exhibited both in the cooling process and in the heating process.

Acknowledgment. This work was financially supported by the National Natural Science Foundation of China (Grant Nos. 10904164 and 10674158) and by the Knowledge Innovation Program of CAS (Grant No. kjcx3.syw.n8).

References and Notes

(1) Bryant, G.; Wolfe, J. *Cryoletters* **1992**, *14*, 23.
(2) Lynch, D. V.; Steponkus, P. L. *Biochim. Biophys. Acta* **1989**, *984*, 267.
(3) Lewis, R. N. A. H.; Sykes, B. D.; McElhaney, R. N. *Biochemistry* **1988**, *27*, 880.
(4) McElhaney, R. N. *Biochim. Biophys. Acta* **1984**, *779*, 1.
(5) Williams, W. P.; Cunningham, B. A.; Wolfe, D. H.; Derbyshire, G. E.; Mant, G. R.; Bras, W. *Biochim. Biophys. Acta* **1996**, *1284*, 86.
(6) Morris, G. J. *The Effects of Low Temperature on Biological Systems* Grout, B. W. W., Morris, G. J., Eds.; Edward Arnold: London, 1987, pp 120−146.
(7) Barton, P. G.; Gunstone, F. D. *J. Biol. Chem.* **1975**, *250*, 4470.
(8) Ulrich, A. S.; Sami, M.; Watts, A. *Biochim. Biophys. Acta* **1994**, *1191*, 225.
(9) Gleeson, J. T.; Erramilli, S.; Gruner, S. M. *Biophys. J.* **1994**, *67*, 706.
(10) Hu, S. X.; Li, X. H.; Jia, Q. J.; Mai, Z. H.; Li, M. *J. Chem. Phys.* **2005**, *122*, 124712.
(11) Salditt, T.; Li, C.; Spaar, A.; Mennicke, U. *Europhys. J. E* **2002**, *7*, 105.
(12) Xing, L.-L.; Li, D.-P.; Hu, S.-X.; Jing, H.-Y.; Fu, H.-L.; Mai, Z.-H.; Li, M. *J. Am. Chem. Soc.* **2006**, *128*, 1749.
(13) Yuan, B.; Xing, L.-L.; Zhang, Y.-D.; Lu, Y.; Mai, Z.-H.; Li, M. *J. Am. Chem. Soc.* **2007**, *129*, 11332.
(14) Katsaras, J.; Watson, M. J. *Rev. Sci. Instrum.* **2000**, *71*, 1737.
(15) ASTM Standards: D 5023-97. Standard Practice for Maintaining Constant Relative Humidity by Means of Aqueous Glycerin Solutions. ASTM (American Society for Testing and Materials) is an international standards

organization that develops and publishes voluntary consensus technical standards for a wide range of materials, products, systems, and services.

(16) Rand, R. P.; Parsegian, V. A. *Biochim. Biophys. Acta* **1989**, *988*, 351.

(17) Pabst, G.; Amenitsch, H.; Kharakoz, D. P.; Laggner, P.; Rappolt, M. *Phys. Rev. E* **2004**, *70*, 021908.

(18) Mason, P. C.; Nagle, J. F.; Epand, R. M.; Katsaras, J. *Phys. Rev. E* **2001**, *63*, 030902.

(19) Chen, F. Y.; Hung, W. C.; Huang, H. W. *Phys. Rev. Lett.* **1997**, *79*, 4026.

(20) Chu, N.; Kucerka, N.; Liu, Y.; Tristram-Nagle, S.; Nagle, J. F. *Phys. Rev. E* **2005**, *71*, 041904.

(21) Keough, K. M. W.; Kariel, N. *Biochim. Biophys. Acta* **1987**, *902*, 11.

JP909739Y